Magnetization, electrical resistivity and neutron diffraction studies of the $U_2(Ni_{1-x}Pt_x)_2In$ system

Magnetization, electrical resistivity and neutron diffraction studies of the $U_2(Ni_{1-x}Pt_x)_2In$ system

V H Tran†§, A Hoser‡ and M Hofmann‡

† W Trzebiatowski Institute of Low Temperature and Structure Research,
Polish Academy of Sciences, PO Box 1410, 50-950 Wrocław, Poland
‡ Hahn–Meitner Institute, Glienicker Strasse 100, 14-409 Berlin, Germany

E-mail: vhtran@int.pan.wroc.pl

Abstract. X-ray powder diffraction, magnetization, electrical resistivity and neutron diffraction experiments were performed on the dense Kondo system $U_2(Ni_{1-x}Pt_x)_2In$. Up to $x \leqslant 0.5$ the alloys crystallize in a tetragonal structure with space group $P4/mbm$ while for $x \geqslant 0.6$ they crystallize in space group $P4_2/mnm$. The observed structural change coincides with the magnetic–nonmagnetic crossover in the system. In the concentration range $0 \leqslant x \leqslant 0.5$, an antiferromagnetic ordering occurs, characterized by a noncollinear arrangement of the magnetic uranium moments in the tetragonal basal plane. In addition, for $x = 0$ and 0.2 a commensurate magnetic ordering is formed with a propagation vector $\boldsymbol{k} = (0, 0, 0.5)$ while for $x = 0.5$ an incommensurate one with $\boldsymbol{k} = (0, 0, 0.5 \pm \tau)$, $\tau = 0.06$ is found. In the concentration range $0.6 \leqslant x \leqslant 1.0$ no magnetic ordering down to 1.7 K is observed. The bulk and neutron scattering data exhibit features attributed to the interplay of the Kondo effect and magnetic exchange interactions. For interpretation of the magnetic behaviour of the $U_2(Ni_{1-x}Pt_x)_2In$ alloys, a strong modification of the density of states at the Fermi surface has been invoked.

1. Introduction

In the recent years, the ternary intermetallic uranium compounds with the chemical formula U_2T_2M where T is a transition metal, M is In or Sn have attracted considerable attention. There are several reasons why these materials make an excellent field to perform research. First, these alloys crystallize either in the U_3Si_2-type structure (space group $P4/mbm$) [1, 2] or in its variant the Zr_3Al_2-type (space group $P4_2/mnm$) [3, 4], belonging to a large family of tetragonal structure compounds. Secondly, these compounds present a variety of complex magnetic structures [5–9] and exhibit exciting physical phenomena, such as insulating Kondo [10] or heavy-fermion behaviour [11].

Studies of the U_2T_2M family of compounds (2:2:1) indicate that the nature of the ground state of these compounds depends sensitively on the hybridization of 5f electrons with the conduction electrons. Based on this hybridization effect, one can explain the evolution of the magnetic behaviour from paramagnetic to the lowest temperature studied (U_2Co_2In, U_2Fe_2Sn) through spin fluctuation (U_2Co_2Sn, U_2Rh_2In) to antiferromagnetic (U_2Ni_2In, U_2Ni_2Sn, U_2Pd_2In, U_2Pd_2Sn) at low temperatures [5–9, 12, 13]. The band structure calculations of these 2:2:1 compounds, performed by Diviš *et al* [11, 14], based on the local density approximation (LDA), have shown a good consistency between the observed properties and variations in

§ Corresponding author.

the electronic structures of most 2:2:1 compounds. However, the nonmagnetic heavy-fermion behaviour of U_2Rh_2In and U_2Pt_2In cannot be described by the LDA-type calculations. Indeed, these two compounds are located on the magnetic/nonmagnetic border line, when plotting their magnetic ordering temperatures versus the square of the calculated f–d hybridization matrix elements [13]. Moreover, this plot resembles the Doniach phase diagram for a Kondo lattice [15] and suggests a competition between magnetic exchange and the Kondo-type interactions.

In this paper, we present for the first time the results of x-ray diffraction, magnetization, electrical resistivity and neutron powder diffraction measurements on the $U_2(Ni_{1-x}Pt_x)_2In$ solid solutions. Since the substitution of Ni by Pt leads to an increase in the unit cell volume, we can just study the modification in the f–d hybridization, mostly driven by the chemical pressure effect.

The two end members of the solid solutions have already been investigated. For U_2Ni_2In ($a = 7.374$ Å, $c = 3.572$ Å [1]), the specific heat [8], dc magnetic susceptibility [12], ac magnetic susceptibility [13] and electrical resistivity [8, 16, 17] measurements were performed. All these experiments have indicated the presence of an antiferromagnetic (AF) order below $T_N = 14$ K. Neutron diffraction experiments [7, 8, 18] have allowed the determination of the magnetic structure, characterized by a magnetic propagation vector $k = (0, 0, 0.5)$. On the other hand, the magnetic susceptibility study made on a polycrystalline U_2Pt_2In sample ($a = 7.679$ Å, $c = 3.703$ Å [1]) has revealed the important role of spin-fluctuation effects in the nonmagnetic ground state of this compound [11]. Furthermore, the heavy-fermion (HF) behaviour characterized by an extreme enhancement in the electronic contribution to the specific heat ($\gamma(0) = 850$ mJ K^{-2} mol^{-1}) has been reported [11]. In addition, the electrical resistivity [19] and magnetoresistance [20] studies on the polycrystalline samples have indicated a non-Fermi-liquid (NFL) behaviour at low temperatures. Also, the electrical resistivity [4] and specific heat [21] measurements recently performed on a single crystal of U_2Pt_2In ($a = 7.694$ Å, $c = 7.367$ Å [4]) have confirmed the NFL behaviour of this compound.

2. Experiment

Polycrystalline samples of the solid solutions $U_2(Ni_{1-x}Pt_x)_2In$ ($x = 0$, 0.1, 0.2, 0.3, 0.4, 0.5, 0.6, 0.7, 0.9 and 1) were synthesized by arc-melting the constituent elements under a high-purity argon atmosphere. Larger samples (≈ 12 g) for neutron diffraction experiments were prepared in an induction furnace. The purity of the starting elements was 99.95 at.% U, 99.99 at.% Ni and Pt and 99.999 at.% In. During melting the weight loss was negligible (less than 0.5% weight). The quality of the samples was checked by means of x-ray powder diffraction. The quantity of impurity phases does not exceed 2% weight.

Magnetization (M) measurements were carried out in the temperature range 1.7–300 K and in magnetic fields (B) up to 5 T, using a SQUID magnetometer (Quantum Design MPMS-5 type). In these measurement powdered samples were used to minimize the texture effects existing in polycrystalline samples.

Electrical resistivity was measured using a standard four-probe method dc technique in the temperature range 4–300 K. A current of 10 mA was applied on bar-shaped samples of typical dimensions $1 \times 1 \times 5$ mm^3. Electrical contacts were established by indium. The voltages were measured to an accuracy of 10 nV, using a Keithley 181 voltmeter. The regulation of temperature was accomplished with an Oxford Instruments ITC503 controller. The absolute accuracy of the measurements was of the order of 5%, depending mainly on the error caused by the geometrical factor.

Neutron diffraction experiments were performed on two samples with $x = 0.2$ and 0.5, using the diffractometer E6, installed at the Hahn–Meitner Institute, Berlin (wavelength

$\lambda = 2.42$ Å). Neutron diffraction diagrams were collected at various temperatures from 1.7 to 25 K. The neutron diffraction intensities were analysed with the Rietveld-type FULLPROF program [22]. The scattering lengths employed in the refinement were $b_U = 0.8417 \times 10^{-12}$ cm, $b_{Ni} = 1.0300 \times 10^{-12}$ cm, $b_{Pt} = 0.9600 \times 10^{-12}$ cm and $b_{In} = 0.4070 \times 10^{-12}$ cm, taken from [23]. In the refinement of the magnetic structure, the magnetic form factor of U^{3+} calculated in the dipolar approximation from $\langle j_0 \rangle$ and $\langle j_2 \rangle$ [24] was used.

3. Results and analysis

3.1. Crystal structure

The x-ray powder patterns for all studied samples showed mainly reflections characteristic of a tetragonal unit cell. Two possible types of structure, namely U$_3$Si$_2$ and Zr$_3$Al$_2$, had to be taken into account. For samples with x up to 0.5, we could index all observed reflections assuming the first type of structure, while for compositions with $x > 0.5$ some new reflections appeared, which required a doubling along the c-axis. This means that the Pt-rich compounds adopt the Zr$_3$Al$_2$-type structure. As reported previously [1,4], a polycrystalline U$_2$Pt$_2$In sample crystallizes in the U$_3$Si$_2$-type structure, whereas a single-crystalline one occurs in the tetragonal Zr$_3$Al$_2$-type structure [4].

The neutron powder diffraction patterns obtained at 15 K for $x = 0.2$ and 0.5 confirm the tetragonal U$_3$Si$_2$-type structure. The refinement of the nuclear intensities performed for these samples leads to a reliability factor R_B of 8.5 and 7.3%, respectively. The refinement results are listed in table 1. Comparing with the results for U$_2$Ni$_2$In (see table 1), there is an increase in both the lattice parameters a and c, but almost no change occurs in the free values of atomic parameters.

Table 1. Crystallographic data for solid solutions U$_2$(Ni$_{1-x}$Pt$_x$)$_2$In, $x = 0.2$ and 0.5.

	0 [7]	0.2	0.5
a (Å)	7.381 (5)	7.462 (5)	7.611 (3)
b (Å)	3.571 (1)	3.618 (3)	3.655 (2)
X_U	0.1816 (13)	0.1722 (18)	0.1775 (15)
X_T	0.3765 (11)	0.3760 (15)	0.3725 (11)
R_B (%)	7.0	8.5	7.3

3.2. Magnetization

Magnetic susceptibility ($\chi = M/B$) measurements have been performed on all the U$_2$(Ni$_{1-x}$Pt$_x$)$_2$In samples prepared. Some representative data of the low-temperature susceptibility, measured in magnetic fields of 0.5 T and 2 T, are shown in figure 1. As this figure illustrates, the compositions with x up to 0.5 behave alike, showing a sharp maximum in their temperature dependencies of the susceptibility $\chi(T)$. This maximum indicates the onset of an antiferromagnetic ordering. In this work, the Néel temperature, T_N, is determined as a maximum in the derivative $d\chi(T)/dT$. For U$_2$Ni$_2$In, the T_N-value of 14.3 K determined here is in good agreement with that reported previously [11–13]. For the other compositions, the value of T_N rapidly decreases with initially increasing concentration of Pt. For instance $T_N = 12.1$ K for $x = 0.1$, and 11.7 K for $x = 0.2$. However, for the $x = 0.2$ samples, the value of T_N is practically independent of x, and amounts to about 11.5 K.
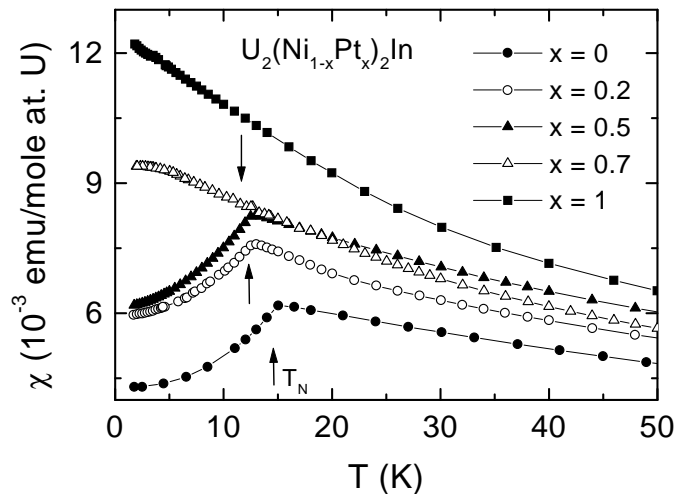
Figure 1. Temperature dependence of the magnetic susceptibility χ of the solid solution $U_2(Ni_{1-x}Pt_x)_2In$. Arrows indicate the Néel temperature T_N. The data for x up to 0.5 were taken at $B = 0.5$, while for $x > 0.5$ at 2 T.

Surprisingly, the alloys with $x > 0.5$ show no χ-anomaly indicating the lack of any magnetic phase transition down to 1.7 K. Thus, we can say a sudden vanishing in the magnetic order occurs between $x = 0.5$ and 0.6 in the $U_2(Ni_{1-x}Pt_x)_2In$ system. For the Pt-richer compositions, a small ferromagnetic component is detected in the $\chi(T)$ curves. This component probably arises due to short-range U–U interactions or to the presence of a small amount of a ferromagnetic impurity like UPt, as previously found in polycrystalline U_2Pt_2In samples by a number of researchers [11, 12]. We argue below that this ferromagnetic contribution to the susceptibility measured at respectively high fields, for instance at 2 T, may be negligible. Indeed, the susceptibility value of U_2Pt_2In at 1.7 K is comparable with the value obtained on a single crystal ($\chi_{\parallel} = 11.9 \times 10^{-3}$ emu mol^{-1}/atom U) [4]. Wilson and other authors [25] demonstrated that the susceptibility of Kondo compounds attains at zero temperature a constant value proportional to the inverse Kondo temperature, T_K. The latter is a measure of the electronic density of states by a relation $\Gamma \approx k_B T_K$, where Γ is the bandwidth of the Kondo resonance at the Fermi energy. Therefore, one can suspect that the tendency to saturation of the susceptibility and its enhancement at low temperatures observed in our case may have the same origin as in Kondo compounds. Furthermore, in the investigated system, the $\chi(T \rightarrow 0)$ value magnifies with increasing x (see figure 1), suggesting an enhancement of the electronic density of the states. The enhancement reaches its largest value in U_2Pt_2In, for which the HF behaviour for this compound may be established without doubt.

Figure 2 shows the magnetization of several $U_2(Ni_{1-x}Pt_x)_2In$ compositions as a function of the magnetic field, $M(B)$. A linear behaviour in this function is observed for the $x \leqslant 0.5$ samples over the measured field range. The samples with $x \geqslant 0.7$ exhibit traces of a ferromagnetic component, which saturates in the magnetic field above 1 T. As one can infer from the remanence values (figure 2), the contribution of ferromagnetic impurities usually does not exceed 1% weight. Furthermore, the linearity in the magnetization between 1 and 5 T indicates that the susceptibility measured at 2 T is sufficient to be in the high-field limit. In other words, one can even neglect the contribution of the ferromagnetic component in the $2T-\chi(T)$ data taken at low temperatures.
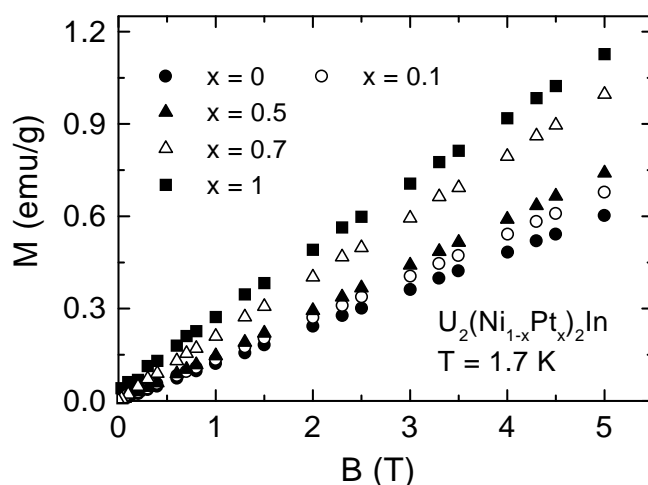
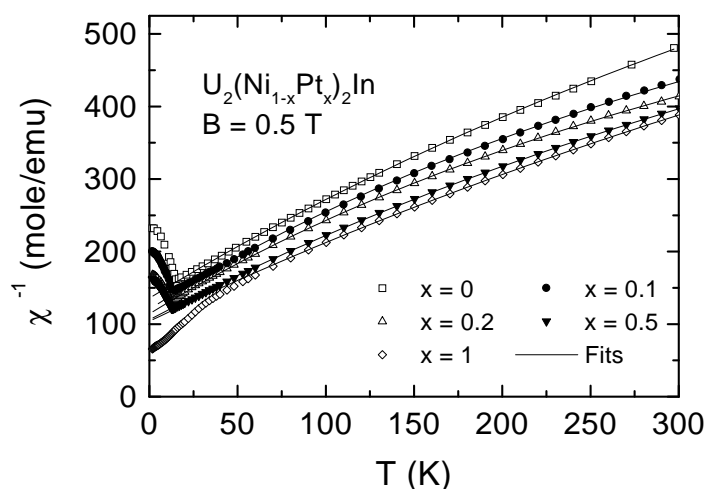**Figure 2.** Magnetization measured at 1.7 K and in magnetic fields up to 5 T.

Figure 3. Reciprocal magnetic susceptibility as a function of temperature.

Figure 3 displays the inverse susceptibility as a function of temperature for some selected $U_2(Ni_{1-x}Pt_x)_2In$ samples. The susceptibility above 75 K can be analysed only by a modified Curie–Weiss law: $\chi(T) = \chi_0 + C/(\Theta_p - T)$. It appears that the effective magnetic moment, μ_{eff}, calculated on the basis of this law, increases steadily over all the compositions from 2.1 μ_B/atom U for U_2Ni_2In to 2.6 μ_B/atom U for U_2Pt_2In. Thus, these values are very close to those reported previously [12]. From the data we can infer the remarkable point that the observed value of the paramagnetic Curie temperature, Θ_p, is more negative than one could expect from the contribution of the magnetic exchange interactions only. For instance, for pure U_2Ni_2In with $T_N = 14$ K, $\Theta_p = -82$ K, while for the Pt-rich compounds, despite their nonmagnetic ground state character, Θ_p tends to be more negative and reaches $\Theta_p = -110$ K for U_2Pt_2In. Such observed behaviour indicates the existence of a Kondo-like effect, which gives rise to the large negative value of Θ_p. Apart from that, one can relate these negative Θ_p-values to the influence of the crystal field on the uranium ions as well.
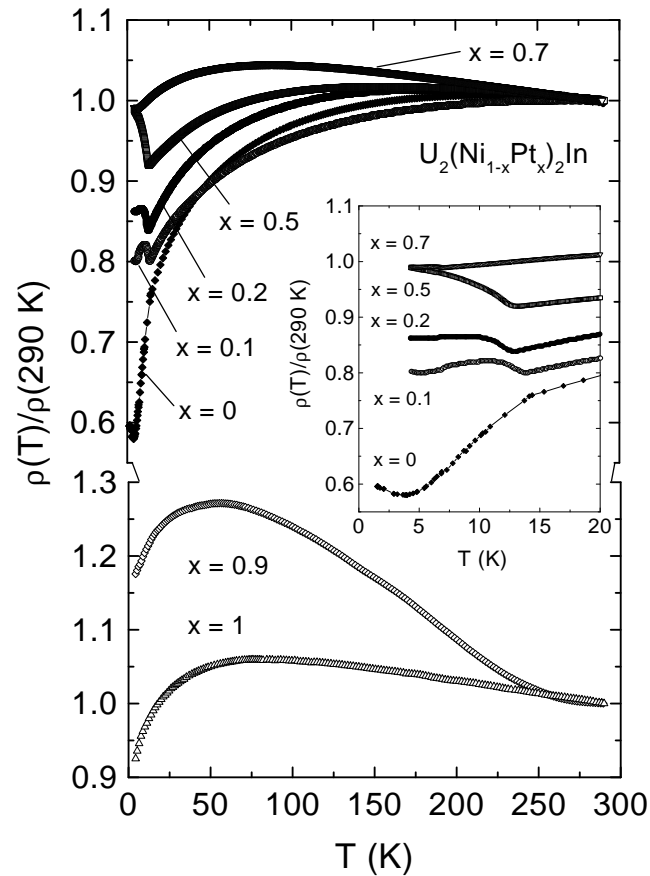
Figure 4. Temperature dependence of the electrical resistivity ρ. The inset shows the resistivity behaviour below 20 K.

3.3. Electrical resistivity

Figure 4 displays the electrical resistivity of selected $U_2(Ni_{1-x}Pt_x)_2In$ samples as a function of temperature. For U_2Ni_2In, the overall behaviour of the resistivity agrees well with that reported in earlier studies [8, 16, 17]. As can be seen from the inset of figure 4, a drop in $\rho(T)$ for U_2Ni_2In appears at 14 K owing to the onset of the antiferromagnetic order. The resistivity of this compound is characterized also by a minimum at 3.8 K. This unusual feature has previously been observed, e.g. for the U-substituted alloys $U_{1-x}Th_xRu_2Si_2$ [26], for which the resistivity behaviour has been explained as being an impurity Kondo-hole effect. On the other hand, within the theory developed by Cornut and Coqblin [27] for the Ce-based Kondo lattice, the low temperature logarithmic behaviour of the resistivity should occur due to the Kondo scattering from the CF ground state. In the U_2Ni_2In compound, a satisfactory fit of the experimental resistivity data below 7 K to the equation $\rho(T) = \rho_0 + AT^2 - C \ln T$ suggested the presence of incoherent Kondo scattering [17].

The substitution of Ni by Pt strongly affects the resistivity behaviour of $U_2(Ni_{1-x}Pt_x)_2In$. It is observed that for the Pt-doped samples with x up to 0.5, a minimum of the resistivity appears, always close to the Néel temperature. The increase in the electrical resistivity at temperatures below T_N was previously obtained in other U compounds, e.g. UCu_5 [28], URu_2Si_2 [29],

UPtGe [30]. A very similar increase in $\rho(T)$ has been shown in pure Cr metal [31], in which an itinerant electron spin density wave transition is expected to occur with a partial gap in the conduction band. Furthermore, theoretical considerations by Elliott and Wedgwood [32] indicate that the resistivity jump below T_N can be a measure of the band energy gap at the magnetic superzone boundary. The substitution of Ni by Pt in $U_2(Ni_{1-x}Pt_x)_2In$ also increases the ratio $\rho(4.2\ K)/\rho(290\ K)$ of samples. This effect may be explained by an increase of the atomic disorder scattering. However, we should take into account the influence of the Kondo effect, which grows gradually with increasing Pt content. The latter interpretation is in line with the resistivity behaviour at high temperatures. It is relevant to the occurrence of a broad maximum at T_{max} and a negative value in the derivative, $d\rho(T)/dT$ above this maximum. One observes that with increasing Pt concentration, the temperature range of the negative $d\rho(T)/dT$-derivative becomes wider, and the ρ-maximum observed at T_{max} ($\approx$200 K for U_2Ni_2In) shifts down to lower temperature ($\approx$50 K for U_2Pt_2In). In a Kondo lattice system, T_{max} is closely related to T_K [33], i.e. $T_{max} \propto T_K \exp(-1/|JN(E_F)|)$, where $N(E_F)$ is the density of states at the Fermi energy and J is the exchange integral. This means that the Kondo temperature decreases with increasing Pt concentration and is associated with the increasing unit cell volume of the solid solutions investigated. This behaviour is consistent with an evolution from the normal AF state of U_2Ni_2In into the HF state of U_2Pt_2In, for which the small value of T_K is equivalent to an enhancement of the electronic density of the states.

3.4. Magnetic structure

Before we will describe the magnetic structures of the investigated compounds, let us recall in more details two models of the magnetic structure for U_2Ni_2In reported previously [7, 8]. Tran *et al* [7], considering the magnetic U sublattice only, have found a non-collinear magnetic structure with the Γ^3 configuration of uranium magnetic moments [34]. The U magnetic moment was fitted to 0.85(5) μ_B/U at 1.5 K with a reliability factor of 6% [7]. A slightly different model has been proposed by Nakotte *et al* [8]. The authors also assumed the Γ^3 configuration of the uranium atoms, but in addition, they considered the induced Ni moments oriented parallel to the c-axis. Comparing both models, one sees that the latter model gives a slightly better fit to experimental data, namely: $\mu_U = 0.58(2)$ μ_B/U, $\chi^2 = 2.4\%$ to $\mu_U = 0.58(1)$ μ_B/U and $\mu_{Ni} = 0.37(4)$ μ_B/Ni, $\chi^2 = 1.7\%$ [8]. However, recently Martin-Martin *et al* [18] have performed neutron experiments on a single crystal of U_2Ni_2In. It appears that the authors did not detect any moment on the Ni sites, and it seems that the model proposed in [7] has been confirmed. Moreover, the value of the ordered moment on the uranium atoms was found to be 0.92(2) μ_B/atom U, thus corroborating the value reported in [7].

In figure 5 we show the magnetic neutron diffraction pattern obtained for the $x = 0.2$ sample by subtraction of two diagrams taken at 1.2 and 15 K (open circles). This pattern is very similar to that observed previously for U_2Ni_2In [7]. Therefore, this alloy should have the same magnetic structure as U_2Ni_2In. Using a propagation vector $k = (0, 0, 0.5)$, the observed magnetic reflections were indexed as $100/01-1^{\pm}$, $110/11-1^{\pm}$, $200/20-1^{\pm}$ and $210/21-1^{\pm}$. Among the ten possible structures for $k = (0, 0, 0.5)$ [34], the best refinement of the magnetic intensities for the above composition corresponds just to the Γ^3 configuration of the magnetic uranium moments. For purposes of illustration, in figure 5 we show the result of such a fit as a solid line. The difference between the calculated and observed intensities is displayed at the bottom of the figure. One can note that there is a reasonable agreement between the observed and calculated intensities ($R_M < 5.6\%$) and diffraction profiles ($R_f < 5.6\%$) for $\mu_{ord} = 0.79(2)$ μ_B/U.
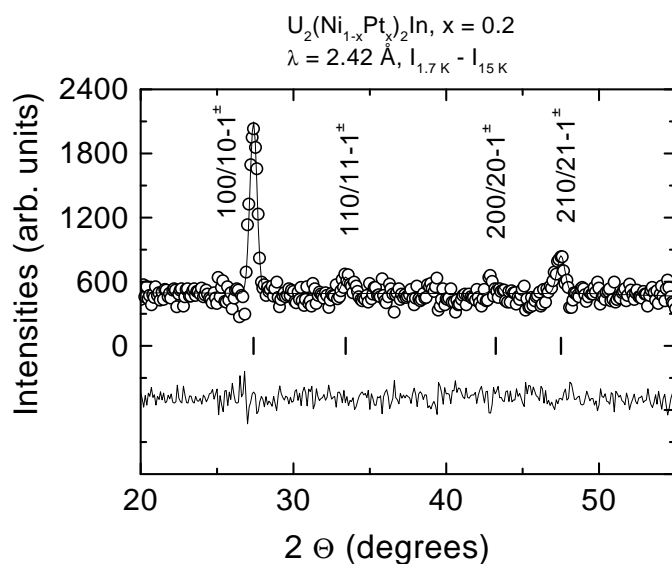
Figure 5. Observed, I_{ob} (open circles), and calculated, I_{cal} (solid line), magnetic patterns as well as the difference between I_{ob} and I_{cal} (solid line at the bottom) for $U_2(Ni_{0.8}Pt_{0.2})_2In$.
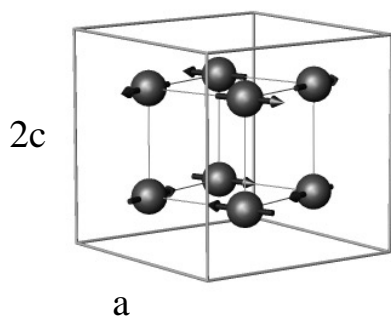

Figure 6. Magnetic structure of $U_2(Ni_{0.8}Pt_{0.2})_{0.2}In$. Only magnetic U atoms are shown.

This time the eventual magnetic ordering of the Ni sublattice in $U_2(Ni_{0.8}Pt_{0.2})_2In$ has also been considered, using the model proposed by Nakotte *et al* [8] for U_2Ni_2In. However, the performed refinements did not yield any significant better result to warrant the inclusion of an additional induced Ni moment. This suggests that in $U_2(Ni_{0.8}Pt_{0.2})_2In$ only the U sublattice is ordered. Of course, we cannot completely exclude induced moment at the Ni sites with its magnitude being e.g. less than 0.1 μ_B, which is the limit of the moment detection in the experiment.

The magnetic structure of $U_2(Ni_{0.8}Pt_{0.2})_2In$ is illustrated in figure 6, taking into account only the U magnetic moments. This structure is commensurate with a propagation vector $k = (0, 0, 0.5)$, and therefore the magnetic unit cell can be described by doubling the *c*-axis with respect to the nuclear cell. The magnetic moments in the basal plane are directed along the C_{2v}-axis, forming a non-collinear spin arrangement. However, when moving from plane to plane the direction of the magnetic U moments reverses, indicating that the coupling between the uranium moments in the adjacent planes is antiferromagnetic.

Figure 7 presents the magnetic neutron diffraction patterns of the $x = 0.5$ sample. These are the differences of diagrams collected at 1.7, 5 and 10 K from that at 15 K. As seen, there are
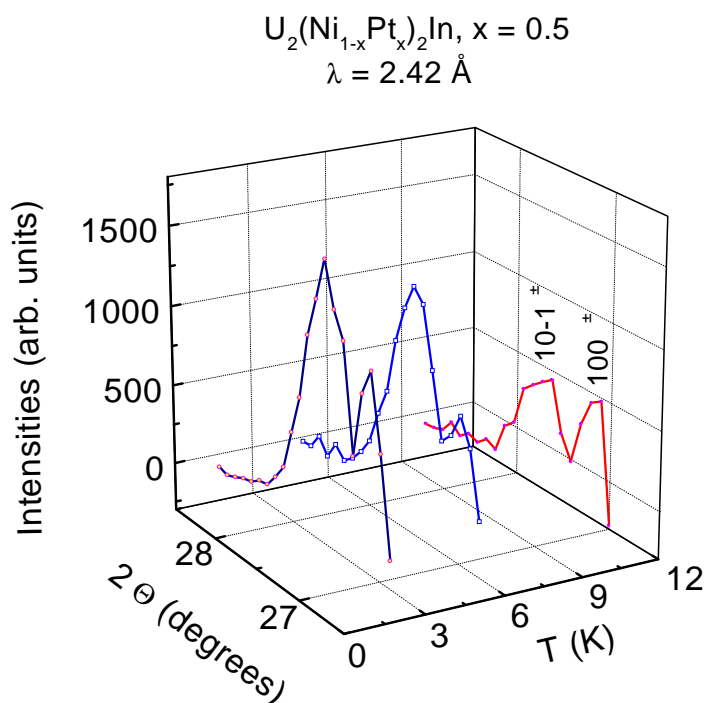
Figure 7. Magnetic patterns of $U_2(Ni_{0.5}Pt_{0.5})_2In$ collected at temperatures below 15 K.

same new peaks of magnetic origin, indicating an antiferromagnetic ground state of this alloy. However, the magnetic peaks could not be indexed, based on simple multiples of the nuclear cell, as is the case for the $x = 0.2$ sample. Instead, the magnetic structure of the $x = 0.5$ sample can be described by an incommensurate propagation vector $\mathbf{k} = (0, 0, 0.5 \pm \tau)$, $\tau = 0.06$. There is no satellite of higher order; therefore, we have examined two possible models: a flat spiral and sinusoidally modulated. It was not possible to obtain agreement between observed and calculated magnetic intensities for a flat spiral ($R_M = 22.5\%$). The best refinement was achieved with a sinusoidally modulated structure, in which the arrangement of spins in the *ab*-plane is identical to that found for $x = 0.2$ but with such a modification that the size of moments varies as a sine wave along the *c*-axis with the amplitude $M_U \cos(2\pi kr)$. The calculation performed for the magnetic intensities completed at 1.7 K (figure 8) led to an average value of the magnetic moment $M_U/\sqrt{2}$ of 0.74(2) μ_B/U and a reliability factor of 8.4%.

Like the case of U_2Ni_2In [7], the values of the magnetic U moment for the compositions $x = 0.2$ and $x = 0.5$ are strongly reduced with respect to that of the U^{3+} free ion (3.27 μ_B/U), manifesting itself probably in both the Kondo screening of the magnetic moments and crystal-field effects.

4. Discussion

The magnetization, electrical resistivity and neutron diffraction measurements performed on the solid solutions $U_2(Ni_{1-x}Pt_x)_2In$ reflect several interesting features: (i) the collapse of antiferromagnetic ordering near $x = 0.5$, (ii) the reduced values of the magnetic U moment
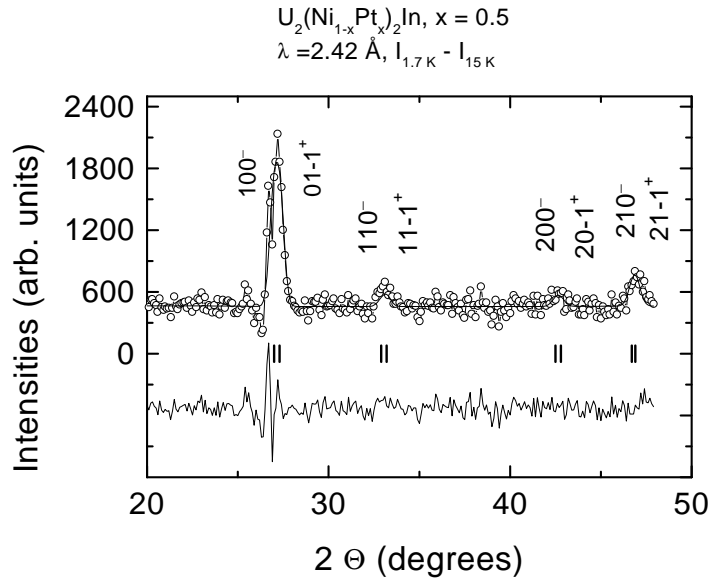
Figure 8. Observed, I_{ob} (open circles), and calculated, I_{cal} (solid line), magnetic patterns as well as the difference between I_{ob} and I_{cal} (solid line at the bottom) for $U_2(Ni_{0.5}Pt_{0.5})_2In$.

in the antiferromagnetic alloys, (iii) the relatively large negative value of Θ_p and (iv) the Kondo-like behaviour of the electrical resistivity $\rho(T)$ in the high temperature range. Based on these findings, we can conclude that there is an interplay of Kondo-like and magnetic exchange interactions in the $U_2(Ni_{1-x}Pt_x)_2In$ system. Here, the Kondo-like behaviour may be interpreted in terms of the volume expansion, where the Kondo temperature is decreased as the Pt concentration is increased. It appears that the Kondo effect is not strong enough in the Ni-rich compositions to screen completely the U moments and thus the antiferromagnetic order persists in compositions with $x \approx 0.5$.

Due to the fact of the sudden disappearance of magnetic ordering in $U_2(Ni_{1-x}Pt_x)_2In$ near $x = 0.5$, the development of the magnetism cannot be explained in terms of the Doniach phase diagram describing the $T_{ord}(x)$ evolution itself [35]. It should be noted that such a collapse of the magnetic order has previously been observed in many intermetallic U-based systems, like $U(In_{1-x}Sn_x)_3$ [36], $Y_{1-x}U_xPd_3$ [37], $Th_{1-x}U_xPd_2Al_3$ [37] and $U_{1-x}Th_xCu_5Al$ [38]. In some of these alloys, a non-Fermi-liquid state has also been found at the concentration close to a quantum critical point [37]. Unfortunately, it is still not clear which physical mechanism drives such non-monotonic changes. Recently, Sereni [39] has considered a number of Ce-based solid solutions containing a magnetic–nonmagnetic crossover. The author distinguishes three groups of compounds: (i) alloys with T_N decreasing continuously to zero, (ii) alloys exhibiting the collapse in magnetism and (iii) alloys where T_N never goes to zero. The difference in the behaviour of alloys belonging to groups (i) and (ii) had been discussed as being associated with a special role of the band electrons. In the first case the magnetic behaviour can be explained in terms of a competition between the Ruderman–Kittel–Kasuya–Yosida (RKKY) interaction and the Kondo effect, according to the scenario of the Doniach description [35], whereas in the second case the polarization of conduction electrons by the local moments is suspected to be very strong, sufficient to weaken the inter-site interaction as the RKKY one. As a consequence, without necessarily implying another mechanism, the magnetic order can break.

In the $U_2(Ni_{1-x}Pt_x)_2In$ system, quite a strong modification in the density of states should be looked for. First, Pt substituting the system drives the AF commensurate structure into an incommensurate one. Secondly, the increase in $\rho(T)$ just below T_N with decreasing temperature for some solid solutions is observed. This means that a superzone gap at the Fermi surface probably appears. The change in the crystal structure type from the U_3Si_2 to Zr_3Al_2 type is further evidence of some reconstruction of the Fermi surface. All these facts imply that the density of states is undoubtedly altered by the alloying effect. Therefore, in order to explain the magnetic behaviour of the $U_2(Ni_{1-x}Pt_x)_2In$ solid solutions we need more detailed data, especially those concerning the electronic structure of this system.

5. Conclusion

By means of x-ray diffraction, magnetization, electrical resistivity and neutron scattering measurements, we have investigated magnetism of a dense Kondo system $U_2(Ni_{1-x}Pt_x)_2In$. We have found that the samples crystallize in the tetragonal structure (space group either $P4/mbm$ or $P4_2/mnm$). The substitution of Ni by Pt in the investigated system modifies the density of states, leading for the Pt-richer compositions to a development of the HF state from the AF state, which is a characteristic of the Ni-richer ones. This change is closely associated with a change in the unit cell volume, which in turn implies the change in the Kondo temperature. An antiferromagnetic order is found in the compositions up to $x = 0.5$. We have found that the $x = 0.2$ sample exhibits the same magnetic structure as U_2Ni_2In [7] with the propagation vector $k = (0, 0, 0.5)$, while the $x = 0.5$ sample has an amplitude-modulated structure with an incommensurate propagation vector with $k = (0, 0, 0.5 \pm \tau)$, $\tau = 0.06$. The uranium moments in these alloys are arranged non-collinearly in the ab-plane and are perpendicularly directed to the propagation vector.

Acknowledgments

References

[1] Peron M N *et al* 1993 *J. Alloys Compounds* **201** 203
[2] Mirambet F, Chevalier B, Fournees L, Gravereau P and Etourneau J 1994 *J. Alloys Compounds* **203** 29
[3] Gravereau P, Mirambet F, Chevalier B, Weill F, Fourès L, Laffargue D, Bourée F and Etourneau J 1994 *J. Matter Chem.* **4** 1893
[4] Estrela P, Pereira L C, de Visser A, de Boer F R, Almeida M, Godinho M, Rebizant J and Spirlet J C 1998 *J. Phys.: Condens. Matter* **10** 9465
[5] Bourée F, Chevalier B, Fournée L, Mirambet F, Roisnel T, Tran V H and Żołnierek Z 1994 *J. Magn. Magn. Mater.* **138** 307
[6] Purwanto A *et al* 1994 *Phys. Rev.* B **50** 6792
[7] Tran V H, Żołnierek Z, Bourée F and Roisnel T 1996 *J. Magn. Magn. Mater.* **161** 270
[8] Nakotte H *et al* 1996 *Phys. Rev.* B **53** 3263
[9] Pereira L C J, Paixao J A, Estrela P, Godinho M, Boudarot F, Bonnet M, Rebizant J, Spirlet J C and Almeida M 1996 *J. Phys.: Condens. Matter* **8** 11 167
[10] Menon L, du Plessis de V and Stydom A M 1998 *Solid State Commun.* **106** 519
[11] Havela L *et al* 1995 *J. Appl. Phys.* **76** 6214
[12] Havela L *et al* 1995 *J. Magn. Magn. Mater.* **140–144** 1367
[13] Tran V H, Żołnierek Z, Zaleski A J and Noël H 1997 *Solid State Commun.* **101** 709

[14] Diviš M, Richter M and Eschrig H 1994 *Solid State Commun.* **90** 99

[15] Doniach S 1977 *Physica* B **91** 231

[16] Pinto R P, Amado M M, Braga M E, Sousa J B, Chevalier B, Laffargue D and Etourneau J 1996 *J. Appl. Phys.* **79** 6355

[17] Strydom A M, du Plessis P de V and Tran V H 1999 *Solid State Commun.* at press

[18] Martin-Martin A, Pereira L C J, Lander G H, Rebizant J, Wastin F, Spirlet J C, Dervenagas P and Brown P J 1999 *Phys. Rev.* B **59** 11 818

[19] Strydom A M and du Plessis P de V 1996 *Physica* B **223/224** 222

[20] Strydom A M and du Plessis P de V 1997 *Physica* B **230–232** 62

[21] Estrela P, de Visser A, de Boer F R, Nieuwenhuys G J, Pereira L C J and Almeida M 1999 *Physica* B **259–261** 409

[22] Rodriguez-Carvajal J 1993 *Physica* B **192** 55

[23] Sears V F 1992 *Neutron News* **3** 26

[24] Freeman A J, Desclaux J P, Lander G H and Faber J Jr 1976 *Phys. Rev.* B **13** 1168

[25] Wilson K G 1975 *Rev. Mod. Phys.* **47** 773
Oliveira L N and Wilkins J W 1981 *Phys. Rev. Lett.* **47** 1553
Rajan V T 1983 *Phys. Rev. Lett.* **51** 308
Bickers N E, Cox D L and Wilkins J W 1987 *Phys. Rev.* B **36** 2036

[26] Lopez de la Torre A, Visani P, Dalichaouch Y, Lee W and Maple M B 1992 *Physica* B **179** 208

[27] Cornut B and Coqblin B 1972 *Phys. Rev.* B **5** 4541

[28] Ott H R, Rudigier H, Felder E, Fisk Z and Batlogg B 1985 *Phys. Rev. Lett.* **55** 1595

[29] Palstra T T M, Menovsky A A, van den Berg J, Dirkmat A J, Kes P H, Nieuwenhuys G J and Mydosh J A 1985 *Phys. Rev. Lett.* **55** 2727

[30] Tran V H, Troć R and Badurski D 1990 *J. Magn. Magn. Mater.* **87** 291

[31] Rapp O, Benediktsson, Åström H U, Arajs S and Rao K V 1978 *Phys. Rev.* B **18** 3665
Fawcett E 1988 *Rev. Mod. Phys.* **60** 209

[32] Elliott R J and Wedgwood F A 1963 *Proc. Phys. Soc.* **81** 846

[33] Lavagna M, Lacroix C and Cyrot M 1982 *J. Appl. Phys.* **53** 2055

[34] Bourée F, Chevalier B, Fournes L, Mirambet F, Roisnal T, Tran V H and Żołnierek Z 1994 *J. Magn. Magn. Mater.* **138** 307

[35] Doniach S 1977 *Valence Instabilities and Related Narrow-Band Phenomena* ed R D Parks (New York: Plenum) p 169
Doniach S 1977 *Physica* B **91** 231

[36] Lin C L, Zhou L W, Crow J E, Guertin R P and Stewart G R 1986 *J. Magn. Magn. Mater.* **54–57** 391
Zhow L W, Lin C L, Crow J E, Bloom S, Guertin R and Foner S 1986 *Phys. Rev.* B **34** 483

[37] Maple M B, Dickey R P, Herrmann J, de Andrade M C, Freeman E J, Gajewski D A and Chau R 1996 *J. Phys.: Condens. Matter* **8** 9773

[38] Troć R, Andruszkiewicz R, Pietri R and Andraka B 1998 *J. Magn. Magn. Mater.* **183** 132

[39] Sereni J G 1998 *J. Phys. Soc. Japan* **67** 1767